International Journal of Signal Processing, Image Processing and Pattern Recognition
Vol.9, No.3 (2016), pp.367-382
http://dx.doi.org/10.14257/ijsip.2016.9.3.32

A Medical Image Fusion Algorithm Based on Multi-channel PCNN in NSCT Domain

Yongmin Guo, Yongdong Huang*

School of Mathematics and Information Science, Beifang University of Nationalities, Yinchuan, 750001, Ningxia, China.
Gsamm520@163.com

Abstract

Medical image fusion plays an important role in clinical applications such as image-guided surgery, image-guided radiotherapy, non-invasive diagnosis, and treatment planning. In order to improve the comprehension of multiple medical image information, we consider the advantage of non-subsampled contourlet transform (NSCT) in multi-scale analysis method and multiple directions and apply it to multi-channel PCNN (m-PCNN). In this paper, a novel medical image fusion method based on m-PCNN in NSCT domain is present. The proposed method exploits the advantage of the multi-scale analysis method and multiple directions of contourlet transform, this algorithm will get the low- frequency and high- frequency sub-bands of the two source medical images by using the NSCT transform, we select different fusion rule in different frequency sub-bands. Low-frequency coefficients are fused by using the average rules, while high-frequency coefficients are fused by inputting to the m-PCNN. The performance of the proposed method is illustrated by using four pairs of medical images as our experimental objects. The experimental results show the superior performance compared with other methods, in both visual effect and objective evaluation criteria.

Keywords: *multi-channel PCNN ; Image fusion ; NSCT*

1. Introduction

Image fusion is a specific algorithm that serves to combine two or more images to form a new image, and then attempt to fuse it into the final composite image with a better description of the scene than any of the individual source image. Recently, image fusion is considered as one of the most promising research topics in the field of image processing, and the technology has formed a rapidly development in civilian and military areas, such as medical image fusion, multi-focus image fusion, infrared target recognition, computer vision.

As the development of the medical, computer technology and biomedical engineering, medical image for clinical diagnosis offers a variety of modal medical images, such as computed tomography, magnetic resonance imaging, positron emission computed tomography, ultrasound images, and so on. As an important medical image processing technology, medical image fusion technology has drawn greater attention in recent years. Studies have shown that the accuracy of CT\MRI image fusion will be more conductive to the implementation of the precise radiotherapy, therefore, many scholars have also made a related research in the multimodal medical image fusion technology, such as contourlet transform [1], DWT [2], dual-PCNN [3], based on principal component analysis (PCA), based on visual, multi-scale geometric analysis algorithm [4,5], etc.

*Corresponding author

Jiao Zhuqing[6] proposed a NSCT domain fusion algorithm, source image which has

ISSN: 2005-4254 IJSIP
Copyright ⓒ 2016 SERSC

been registered is decomposed by using NSCT transform, and then low frequency subband and bandpass subband coefficients are obtained. NSCT based on the theory of contourlet transform has different number of directions at each scale and leads to better frequency selectivity and regularity. PCNN is a biologically inspired neural network based on the work by Eckorn.et al[7], it has the character of global coupling and pulse synchronous of neurons. In 1999, Johnson and Padgete [8]pointed out that there was a great potential for PCNN in the field of image fusion[9]. Researchers have developed some image fusion algorithms based on PCNN[10.11]. Li Meili [12] proposed the fusion algorithm based on NSCT and PCNN and this algorithm was better than NSCT transform[13], an image fusion algorithm based on PCNN is proposed to deal with bandpass subband coefficients of the fusing image obtained by NSCT transform, finally, the fused images are obtained by using inverse NSCT transform on the fused low- and high- frequency coefficients. However, all the image fusion methods using PCNN have the defect that one PCNN cannot finish the whole process of multi-source images and the value of single pixel is used to motivate one neuron in spatial or MSD domain. Zhaobin Wang [14] proposed a m-PCNN model for the first time in 2008, but m-PCNN in spatial or discrete wavelet transform can only capture limited directional information. In this paper, we proposed a novel algorithm based on m-PCNN in NSCT domain, it can not only overcome those defects which can’t deal with various types of medical images, and can retain the clear region and feature information of multimodal image.

The rest of the paper is organized as follows. In section 2, the dual-PCNN is briefly reviewed, and then m-PCNN and its existing problems, and m-PCNN model in NSCT domain are introduced, respectively. In section 3, an image fusion algorithm based on m-PCNN in NSCT domain is described. In section 4, the experimental results and the performance evaluation of various medical image fusion methods are given. Finally, conclusions are summarized.

2. M-PCNN Model in NSCT Domain

2. 1 Dual-PCNN Model

PCNN is a biologically inspired neural network based on the work by Eckhorn et al. , which has the characteristics of the global coupling and pulse synchronization. Pioneering work in the implementation of PCNN was done by Johnson and his colleagues [15–17], it has been proved that PCNN is very suitable for image processing, such as image segmentation, image enhancement, pattern recognition, etc.

The dual-PCNN neuron consists of three parts: an input part (dendritic tree), the linking modulation (information fusion), and the pulse generator [18], as shown in Fig. 1.

 Copyright ⓒ 2016 SERSC

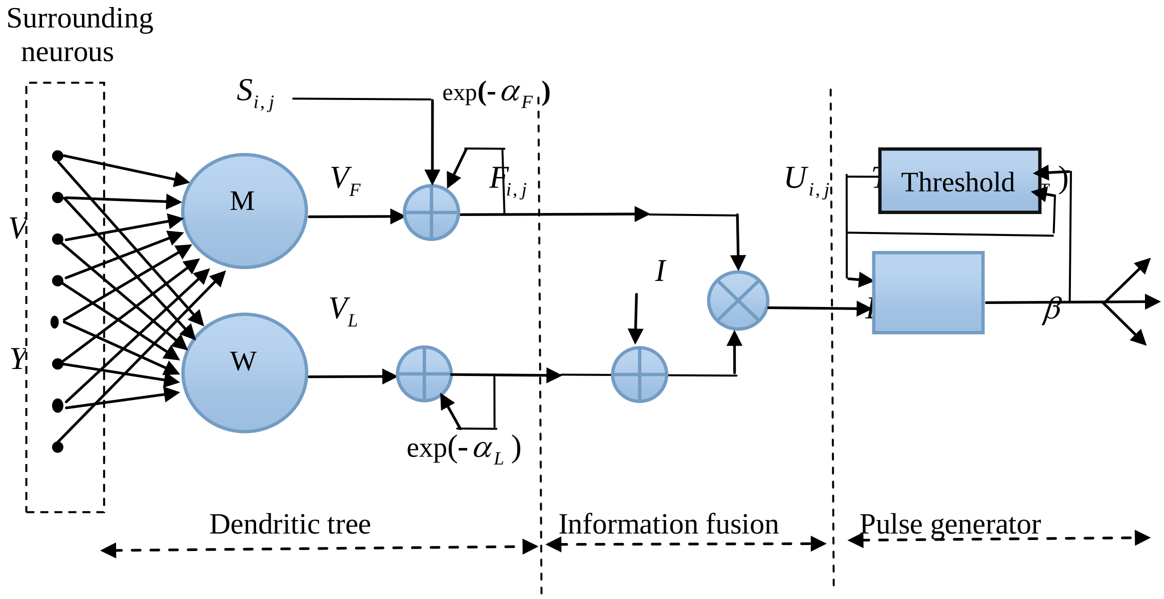

Figure 1. The Neuromime of PCNN

The following expressions describe its mathematical model:

$$H_{i,j}^{A}[n] = S_{i,j}^{A} + \sum_{k,l} w_{ijkl} Y_{kl}[n-1] \tag{1}$$

$$H_{i,j}^{B}[n] = S_{i,j}^{B} + \sum_{k,l} m_{ijkl} Y_{kl}[n-1] \tag{2}$$

$$U_{i,j}[n] = (1+\beta_{i,j}^{A} H_{i,j}^{A}[n])(1+\beta_{i,j}^{B} H_{i,j}^{B}[n]) + \delta \tag{3}$$

$$Y_{i,j}[n] = \begin{cases} U_{i,j}[n] - Sur_{i,j}[n], U_{i,j}[n] > T_{i,j}[n-1] \\ 0, \text{otherwise} \end{cases} \tag{4}$$

$$T_{i,j}[n] = \begin{cases} e^{-\alpha_T} T_{i,j}[n-1], Y_{ij}[n] = 0 \\ V_T, \text{otherwise} \end{cases} \tag{5}$$

In Eqs. (1)- (5) , $H_{i,j}^{A}$ and $H_{i,j}^{B}$ refer to the external input of image A and image B, respectively. $T_{i,j}$ is the firing threshold, the indexes i and j refer to the pixel location in the image, k and l refer to the dislocation in a symmetric neighborhood around one pixel, and n denotes the current iteration (discrete time step), n varies from 1 to N (the total number of iterations), $F_{i,j}$, $L_{i,j}$ are the feeding input and linking input of the i, j neuron, respectively. w_{ijkl} and m_{ijkl} are the synaptic gain strength coefficients. $S_{i,j}$ is the input stimulus, $U_{i,j}$ is the internal state of the neuron, and $\beta_{i,j}$ is the linking strength, $Y_{i,j}$ is the pulse output of the neuron, $Sur_{i,j} = \sum_{k,l} K_{ijkl} Y_{kl}[n-1]$, V_T and α_T are normalized constant and attenuation time, respectively.

2. 2 M-PCNN Model

As we all known that only one stimulus for each neuron is an obstacle for multiple-image fusion using the dual-PCNN. In order to overcome the defect, Zhaobin

Wang proposed a m-PCNN model for the first time, as shown in Fig. 2.

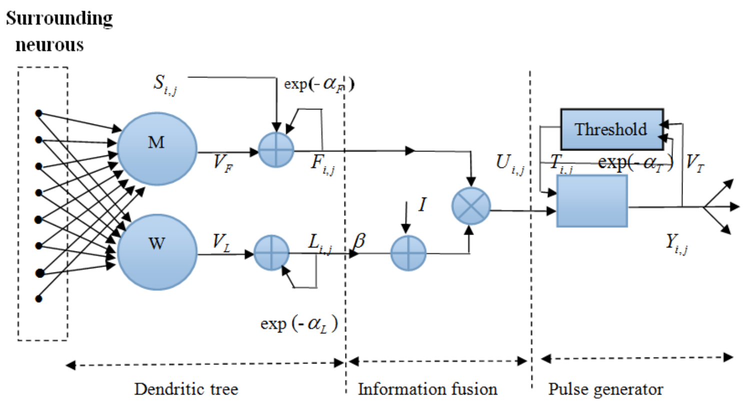

Figure 2. The Neuromime of m-PCNN

It is obvious that there are m input channels in the m-PCNN model; generally, $m > 1$. The model can adjust the number of external input channel according to practical demands compared with the dual-channel PCNN. The following expressions describe its mathematical model:

$$H_{i,j}^{k}[n] = f^{k}(Y[n-1]) + S_{i,j}^{k} \tag{6}$$

$$U_{i,j}[n] = \prod_{k=2}^{K}(1+\beta^{k}H_{i,j}^{k}[n]) + \delta \tag{7}$$

$$Y_{i,j}[n] = \begin{cases} 1, U_{i,j}[n] > F_{i,j}[n-1] \\ 0, \text{otherwise} \end{cases} \tag{8}$$

$$T_{i,j}[n] = \exp(-\alpha_{T})T_{i,j}[n-1] + V_{T}Y_{i,j}[n] \tag{9}$$

Here, H^{k} denotes the channel of the $k-th$ external input, S^{k} is the input stimulus of the $k-th$ channel, k =2, 3,. . . m (m is the total number of external inputs), and $f^{k}(\cdot)$ is the feed function. β^{k} denotes the weighting factor of the $k-th$ channel, usually, $0 < \beta^{k} < 1$, δ is the level factor, other parameters have the same meanings as the above PCNN. Note: In order for the image fusion make sense, external input source images must be registered and all inputs should also have identical resolution.

2. 3 Nonsubsampled Contourlet Transform

Contourlet transform is proposed by DO [19], it is a two-dimensional image representation algorithm, which not only has the multi-scale and time-frequency local feature, but also has the directional feature.

Arthur L. da Cunha et al. proposed the NSCT transform[17]. The structure of NSCT is divided into nonsubsampled pyramid (NSPD) and nonsubsampled directional filter bank (NSDFB), which achieves its shift-invariance property. Images are decomposed based on NSCT transform which are better able to deal with high dimensional singularity, such as contour and texture. Further, the shift-invariance property of NSCT can effectively avoid pseudo-Gibbs phenomena.

NSPD is a shift-invariance filtering structure which explains the multiscale property of NSCT, and is achieved by using two-channel non-subsampled 2D filter banks, we can consider NSPD as the process of eliminating the downsampers and upsampers through Laplacian pyramid and upsampling the filters accordingly. The filters satisfy the following identify:

 Copyright ⓒ 2016 SERSC

$$H_0(z)G_0(z) + H_1(z)G_1(z) = 1 \quad (10)$$

Then the perfect reconstruction is achieved. Where $H_0(Z)$ is the lowpass decomposition filter, $H_1(Z)$ is the highpass decomposition filter, $G_0(Z)$ is the lowpass reconstruction filter, $G_1(Z)$ is the highpass reconstruction filter.

NSDFB is constructed by eliminating the downsamplers and upsamplers of the DFB and upsampling the filters accordingly. In fact, NSDFB is translated to the DFB of the contourlet transform. To obtain multidirectional decomposition, the NSDFBs are iterated to get the next level decomposition all filters are upsampled by a quincunx matrix given by

$$QM = \begin{bmatrix} 1 & 1 \\ 1 & -1 \end{bmatrix} \quad (11)$$

3. Image Fusion Algorithm

Although PCNN has applied to image fusion for several years, in order to make the multi-source image fusion to retain more detail information, here we proposed a medical image fusion algorithm based on m-PCNN in NSCT domain. Our method is shown as follows:

(1) The two registered source medical images are decomposed to obtain a pair of low-frequency sub-images and a number of high-frequency sub-images by using the NSCT transform .

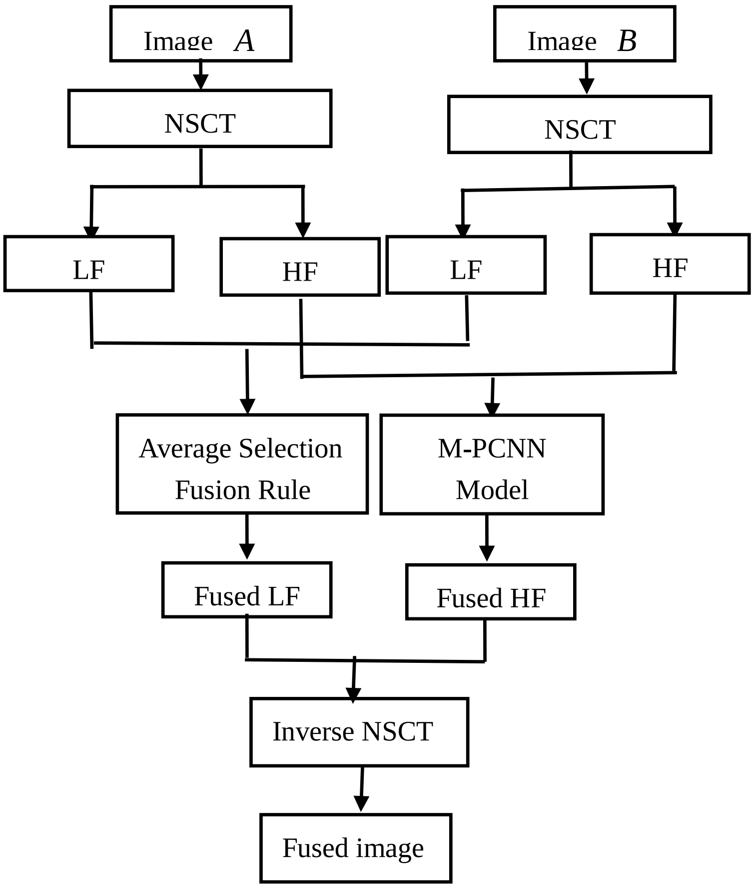

Figure 3. Block Diagram of the Proposed Algorithm

(2) Fused low -frequency coefficients using the average rules.
(3) The high-frequency coefficients of the source medical images are inputted to the m-PCNN.

-M-PCNN parameters are initialized.

-Let S_k denote the high-frequency coefficients of the registered source medical images, $k \geq 2$.

-According to Eqs.(6) and (7), mix the stimuli and feed information from all channels, and output the internal signal U_n.

-According to Eqs.(8) and (9), determine the firing events, and record the number of firing neurons in the current iteration, denoted as C_n.

-$Sum[n] = Sum[n-1] + C_n$, $Sum[n]$ denotes the total number of the fired neurous after the current iteration. $Sum[n-1]$ denotes the total number of the fired neurous before of the current iteration.

-If $Sum[n] < Num$, turn to 2, otherwise, continue.

-Normalize U_n, $U = Normal(U_n)$, where U includes all of the fused high frequency information needed.

(4) Apply inverse NSCT to reconstruct the fused image F.

The block diagram of the proposed algorithm is shown in Fig.3.

4. Experimental Result and Analysis

In this section, we use m-PCNN in NSCT domain to fuse multimodal medical images, mainly consists of two parts: parameter setting, performance evaluation and analysis. So we firstly give parameters of the m-PCNN model, then, in order to testify the feasibility of the proposed method, visual effect and objective evaluation criteria are done. Finally, we illustrate the experiments of different medical images with the proposed method.

4. 1 Parameter Setting

In this experiment, we implemented the proposed method in MATLAB 7. 1. In the m-PCNN, the parameters are set as follows: $\beta^1 = \beta^2 = 0.5$, $M(\cdot) = \mathrm{W}(\cdot) = \mathrm{Y[n-1]} \otimes \mathrm{K}$, $K = [0.1091, 0.1409, 0.1091; 0.1409, 0, 0.1409; 0.1091, 0.1409, 0.1091]$, where $\otimes$ denotes convolution operation, $\delta = 1$; time constant $\alpha_T = 0.012$; and $V_T = 4000$ are selected.

In order to show excellent properties of our method, it is compared with several existing method**s** :wavelet[11], average, pixel take maximum, pixel take minimum, PCA, dual-PCNN[8], m-PCNN[14], NSCT[6], NSCT+PCNN. In the experimental images for each group (Fig4,5,8,9), image (1) and (2) are source images. Image (3) are the fused image using our method, the remained images are obtained by other methods.

4. 2 Performance Evaluation

4.2.1 Visual Effect: In order to evaluate the performance of our method, four group experiments with medical image fusion have been performed. Here we give an explanation for figuers : Figs 4,5,8,9 are experimental results obtained by several methods.

To evaluate objectively the methods mentioned above, we choose mutual information as the objective evaluation. It can be calculated by the following formula:

$$MI(S,F) = H(S) + H(E) - H(S,F) \tag{12}$$

 Copyright ⓒ 2016 SERSC

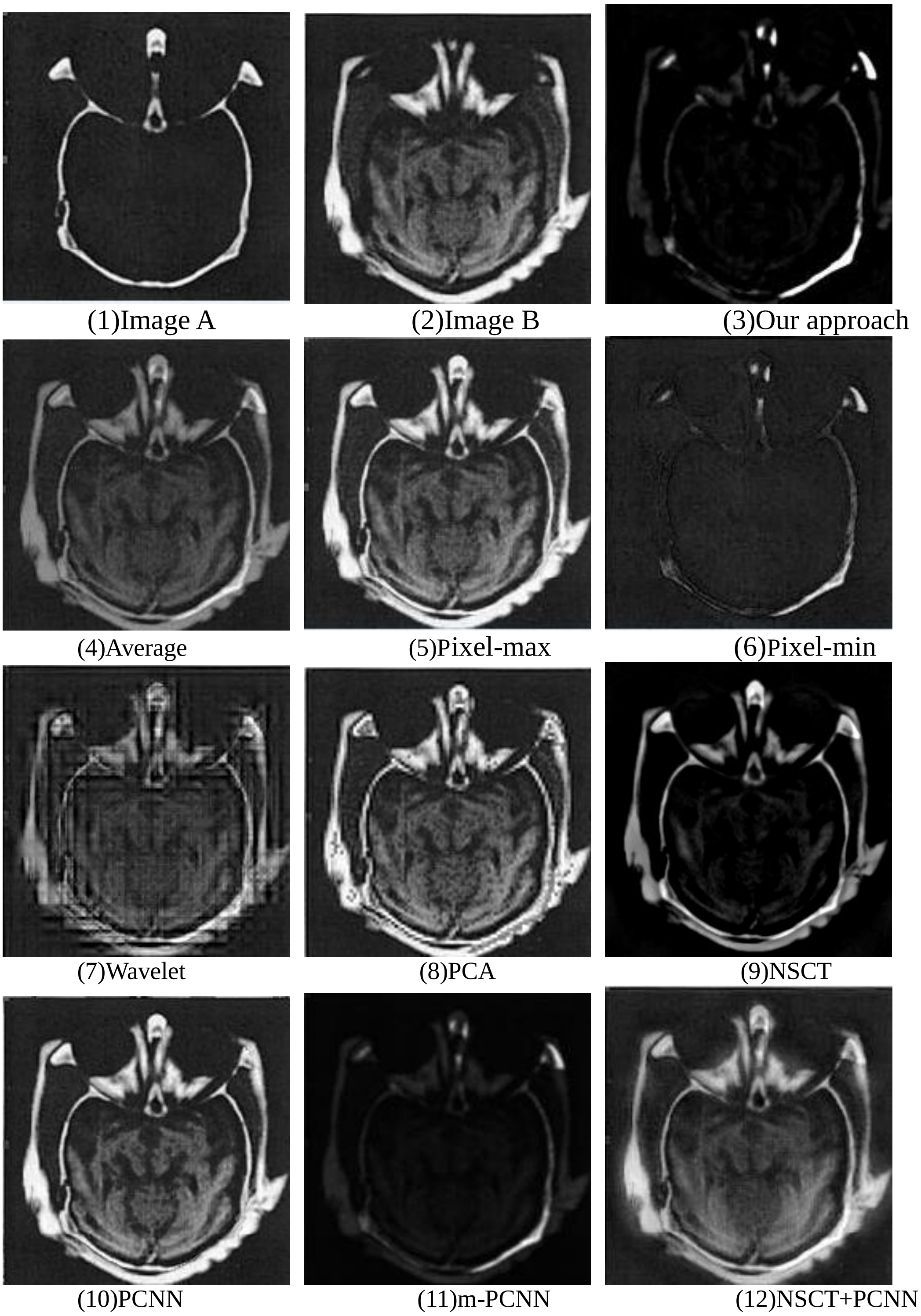

Figure 4. Group 1 Experimental Images:(1)and(2) are Original Images. (3)-(12)are Fused images

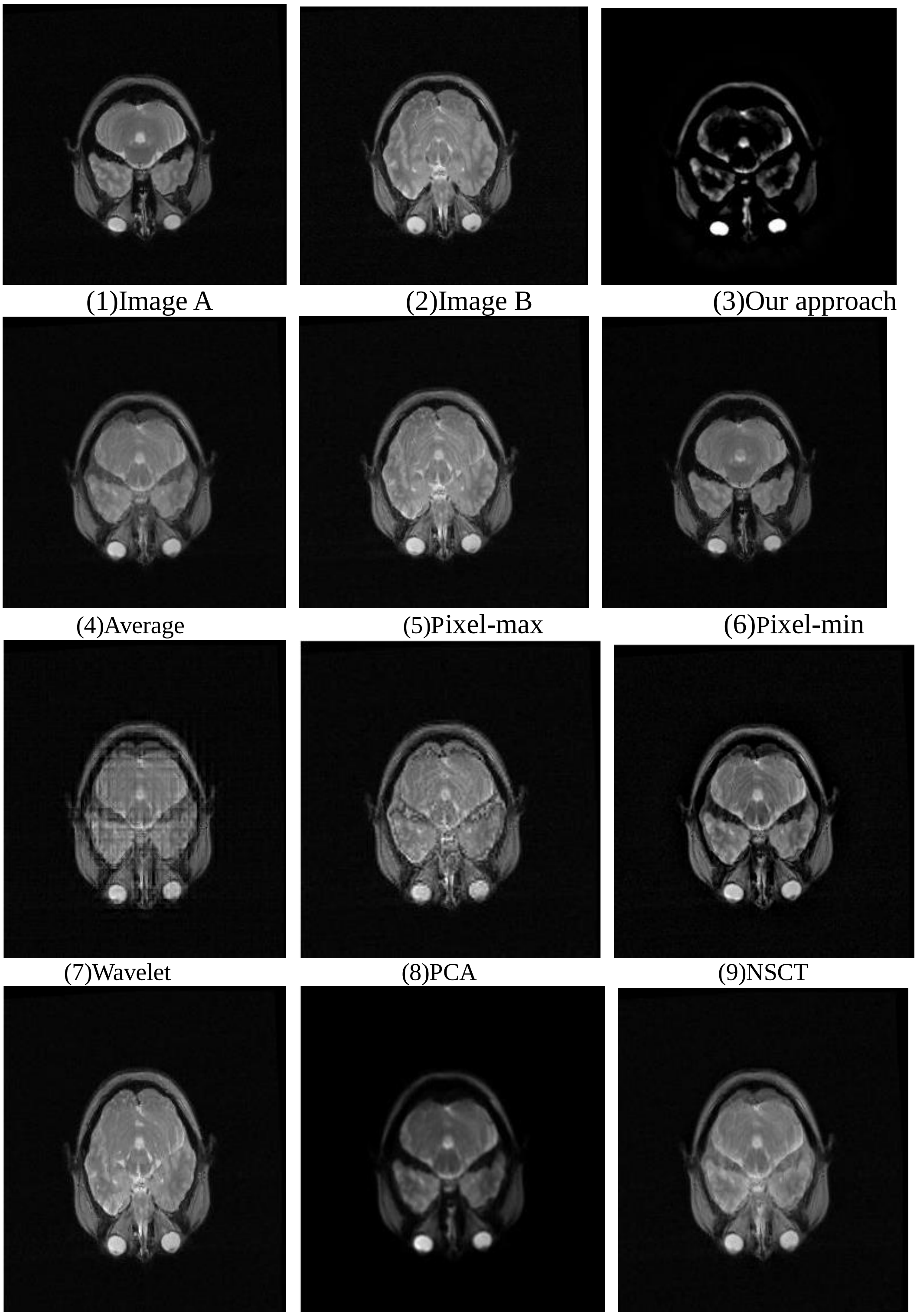

(1)Image A (2)Image B (3)Our approach

(4)Average (5)Pixel-max (6)Pixel-min

(7)Wavelet (8)PCA (9)NSCT

(10)PCNN (11)m-PCNN (12)NSCT+PCNN

Figure 5. Group 2 Experimental Images:(1)and(2) are Original Images (3)-(12)are Fused Images

where $H(\cdot)$ is entropy, $H(S,F)$ is the joint entropy between S and F. It measures the degree of dependence of two images，so the larger the value of mutual information is, the more information of the fusion images obtained from source images, the better the effect

 Copyright ⓒ 2016 SERSC

of fusion there is. Now, we explain the terms in the tables, $\mathrm{MI-AF}$ denotes mutual information between source image A and the fused image F; $\mathrm{MI-BF}$ denotes mutual information between image B and the fused image F; $\mathrm{MI-AB}$ denotes the total of mutual information
and its value is the sum of $\mathrm{MI-AF}$ and $\mathrm{MI-BF}$.

From the visual point of view, it is obvious that : Fig.4(4) does not reflect the information that appears as bright spots; 4(5) and 4(10) seem very similar; 4(6) does not contain the information in image B; 4(7) does not clear and has a lot of stripes; 4(8) contains a lot of noise. However, looking at Fig.4(9), there are also some sharp edges in this figure; 4(12) is blurred, which reduce the image quality. The results of objective assessment are shown in Fig.6 and Table 1. Moreover, (9) and (12) is time consuming.

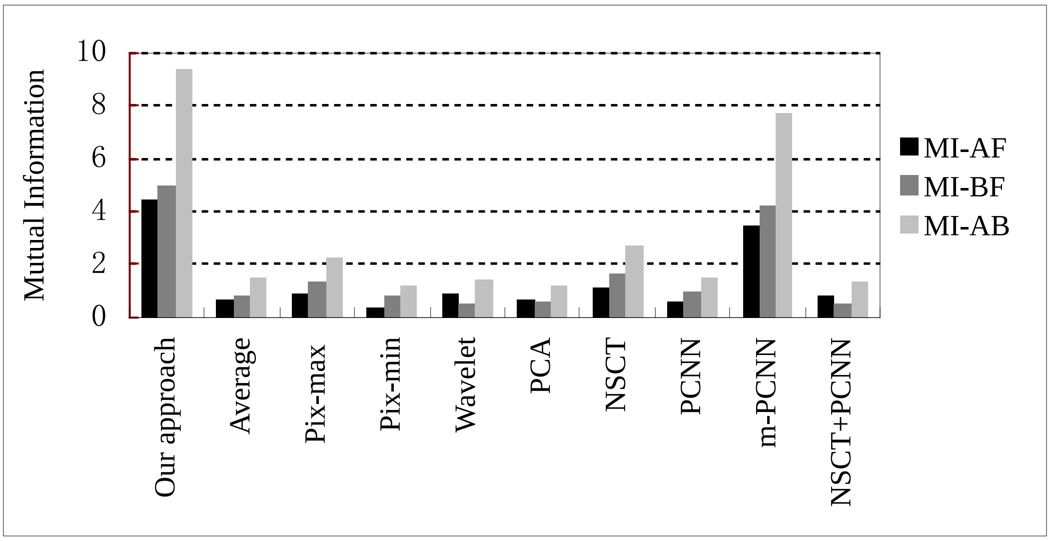

Figure 6. Group 1: Performance of Different Methods

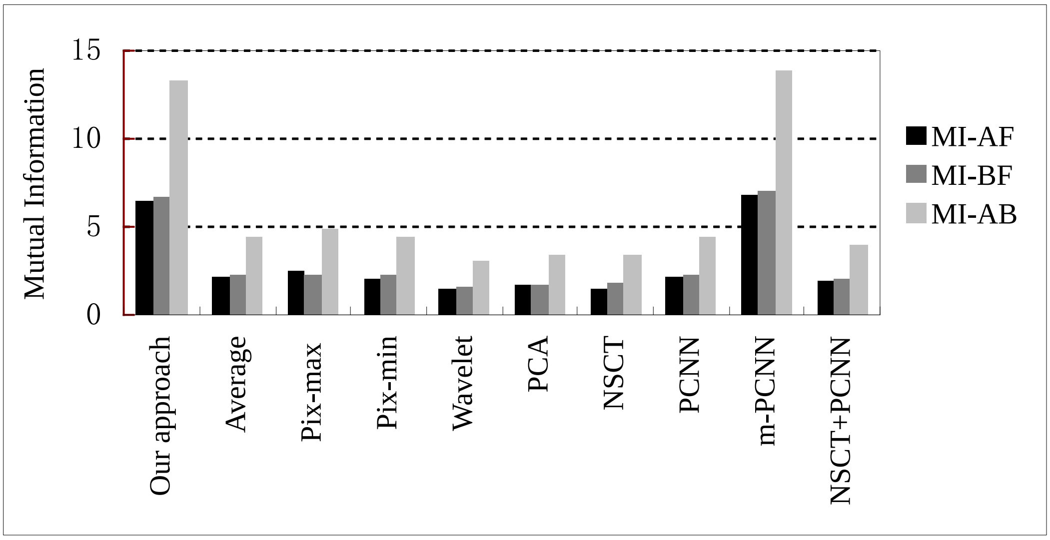

Figure 7. Group 2: Performance of Different Methods

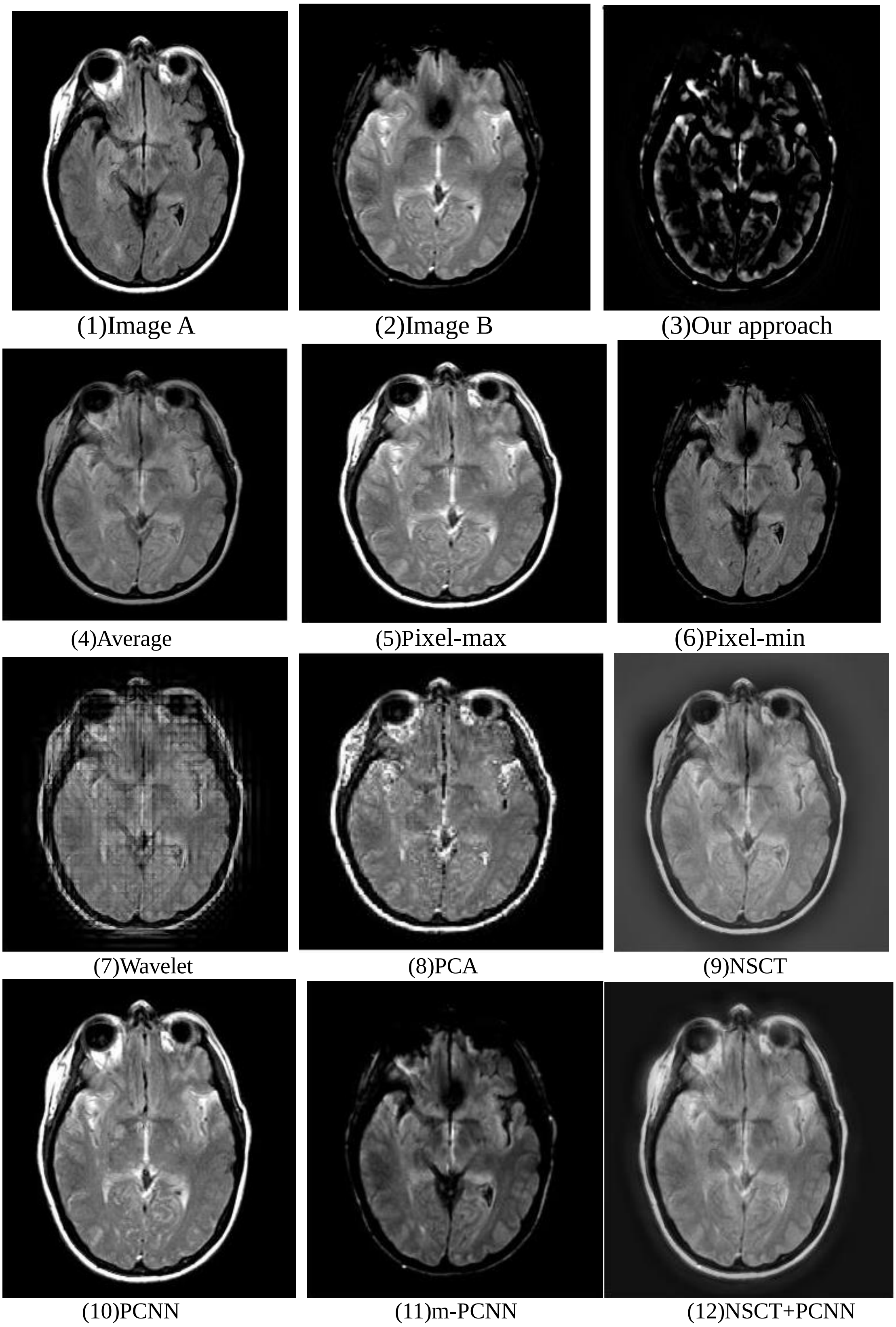

Figure 8.Group 3 Experimental Images:(1)and(2) are Original Images. (3)-(12) are Fused Images

Copyright ⓒ 2016 SERSC

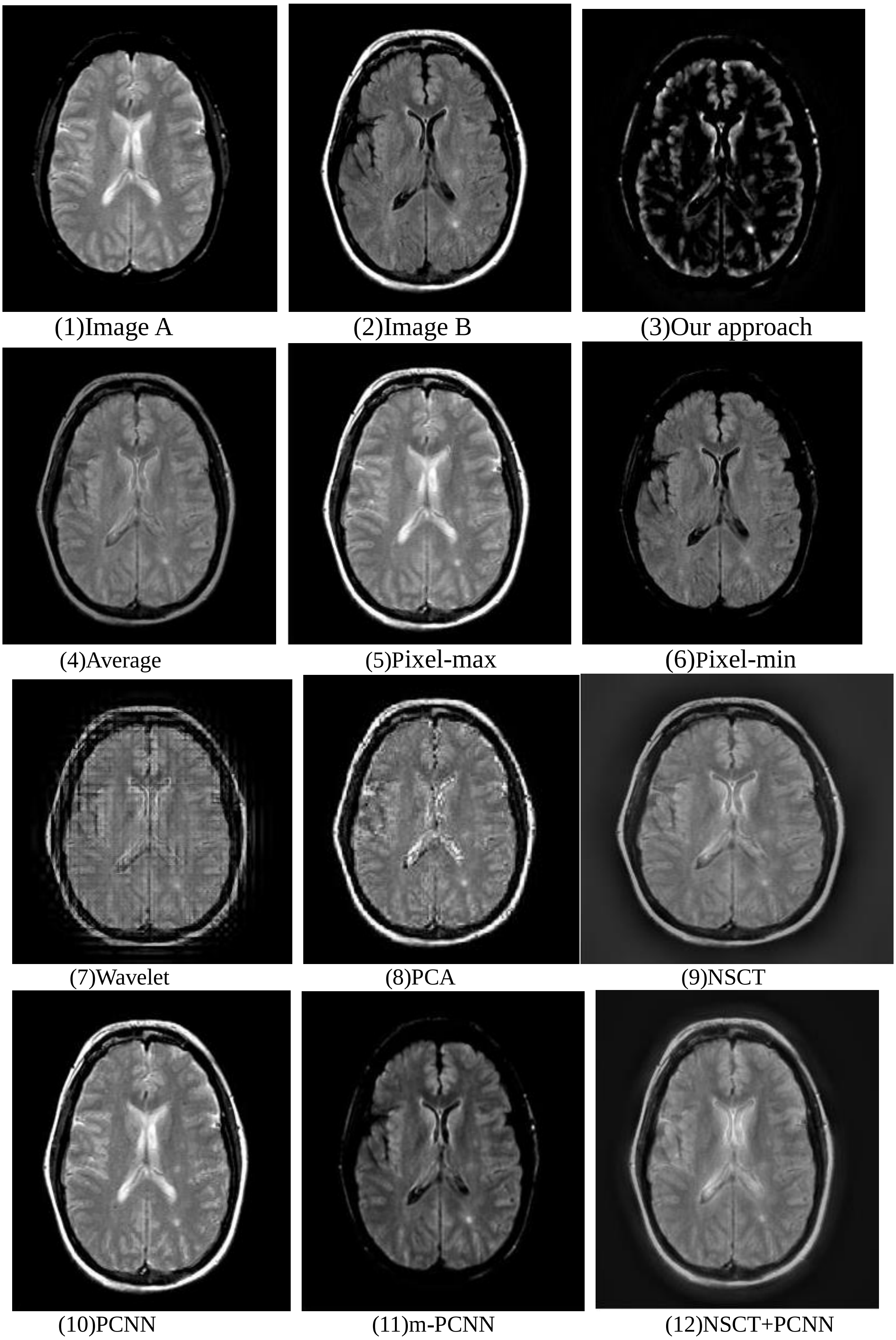

Figure 9. Group 4 Experimental Images:(1)and(2) are Original Images (3)-(12)are Fused Images

For Fig.7, we observe that: 7(4) and 7(11) is blurred. 7(5) and 7(10) does not contain the information in image A; 7(7) and 7(9) contains a lot of stripes ; 7(8) contains a lot of noise; 7(12) does not reflect the information obviously. The results of objective assessment are shown in Fig.7 and Table 2.

It is obvious that: From Fig.8, 8(4) and 8(9) does not reflect the edge information that appears as bright spots; 8(5) does not reflect the detailed information in image A; 8(6) and 8(11) does not contain the information in image A; 8(7) contains a lot of stripes; Fig.8(8) contains a lot of noise; 8(10) does not reflect the information in image A obviously; 8(12) is blurred. The results of objective assessment are shown in Fig. 9 and Table 3.

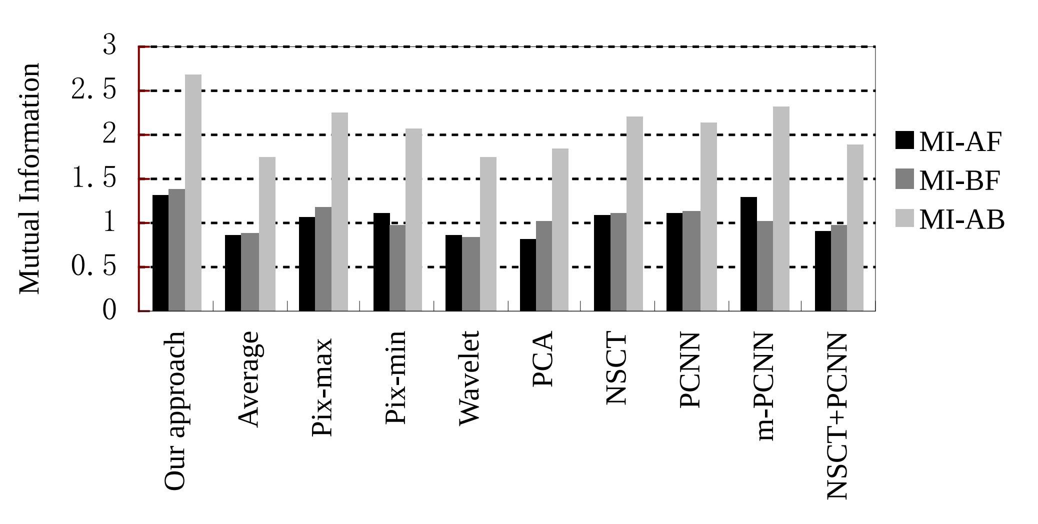

Figure 10. Group 3: Performance of Different Methods

For Fig.9, we can observe that: 9(4) and 9(12) are blurred and have bad edges; 9(5) does not reflect the detailed information in image B; 9(6) and 9(11) does not contain the information in image A and have bad edges; 9(7) contains a lot of stripes; 9(8) contains a lot of noise; 9(10) does not reflect the information in image B obviously; 9(11) can not contain much more detailed information in image A and B. The results of objective assessment are shown in Fig.11 and Table 4.

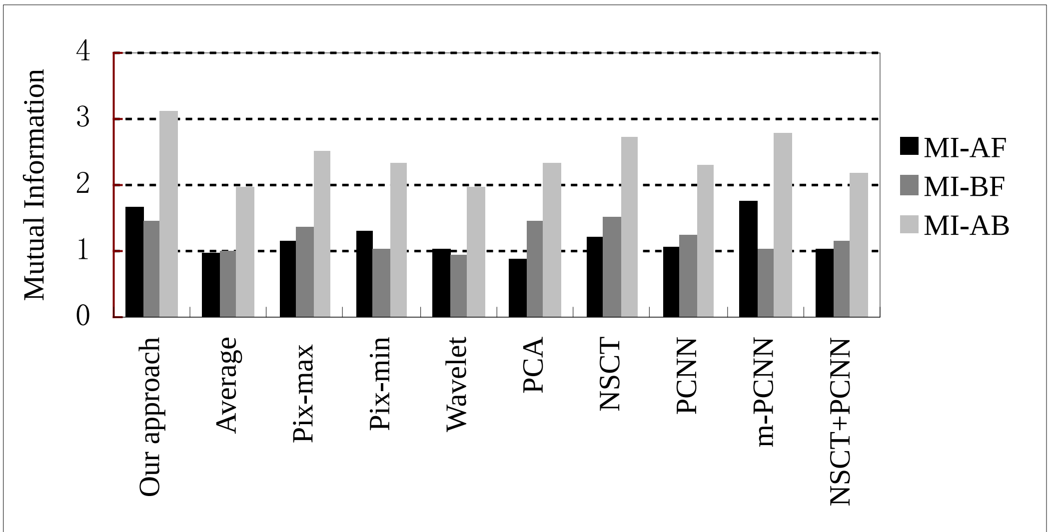

Figure 11. Group 4: Performance of Different Methods

 Copyright ⓒ 2016 SERSC

4.2.2 Objective Standard: For the sake of objectively assessing various methods, we take mutual information as the objective standard to estimate the performance of different methods, the results of various methods is shown as follows.

Table 1. Objective evaluation MI index(Group 1)

Methods	MI_AF	MI_BF	MI_AB
Our approach	4.4194	4.9469	9.3663
Average	0.7002	0.7937	1.4939
Pixel-max	0.9214	1.3389	2.2603
Pixel-min	0.3871	0.8112	1.1983
Wavelet	0.9229	0.5102	1.4331
PCA	0.6677	0.5628	1.2305
NSCT	1.0992	1.6282	2.7281
PCNN	0.5634	0.9445	1.5079
m-PCNN	3.4337	4.2559	7.6932
NSCT+PCNN	0.8016	0.5218	1.3234

Table 2. Objective Evaluation MI Index(Group 2)

Methods	MI_AF	MI_BF	MI_AB
Our approach	6.5392	6.7993	13.3385
Average	2.2202	2.2832	4.5034
Pixel-max	2.5729	2.3237	4.8966
Pixel-min	2.1083	2.3237	4.4320
Wavelet	1.4990	1.6539	3.1529
PCA	1.7013	1.7598	3.4629
NSCT	1.5378	1.9011	3.4389
PCNN	2.1970	2.2660	4.4630
m-PCNN	6.9015	7.0421	13.9436
NSCT+PCNN	1.9291	2.0859	4.0150

Table 3. Objective Evaluation MI Index(Group 3)

Methods	MI_AF	MI_BF	MI_AB
Our approach	1.3038	1.3702	2.6740
Average	0.8609	0.8797	1.7406
Pixel-max	1.0627	1.1744	2.2371
Pixel-min	1.0969	0.9612	2.0581
Wavelet	0.8596	0.8447	1.7043
PCA	0.8182	1.0214	1.8423
NSCT	1.0964	1.1053	2.2017
PCNN	1.0013	1.1200	2.1213
m-PCNN	1.2896	1.0096	2.2992
NSCT+PCNN	0.9076	0.9813	1.8889

Table 4. Objective Evaluation MI Index(Group 4)

Methods	MI_AF	MI_BF	MI_AB
Our approach	1.6605	1.4436	3.1041
Average	0.9707	0.9876	1.9583
Pixel-max	1.1440	1.3626	2.5066
Pixel-min	1.2996	1.0132	2.3128
Wavelet	1.0298	0.9298	1.9596
PCA	0.8876	1.4436	2.3312
NSCT	1.2053	1.5223	2.7276
PCNN	1.0549	1.2491	2.3040
m-PCNN	1.7539	1.0181	2.7720
NSCT+PCNN	1.0289	1.1415	2.1704

Tables 1~4 reflect the value of MI of group 1~4, respectively, image A and image B in figs. 4,5,8,9 denote source medical images. Image A in fig.4 is a CT image that shows structures of bone, while image B is a MR image that shows areas of soft tissue. Image A and image B in fig.5,8,9 are a CT and MR images of brains, respectively.

From the data in tables 1-4, we can know that the value of MI of the proposed method is the largest. However, from the table 1, we see that the value of MI of the pixel-min is the smallest, which show that the performance is poor. From the table 2, the value of MI of the wavelet is the smallest, except for our method and m-PCNN, we can see that the values of MI of other eight methods are similar. From the table 3, the value of MI of the wavelet is the smallest, in addition, we can observe that the values of the nine methods except the proposed method are similar. From the table 4, we can see that the value of MI of the average is the smallest, the values of the nine methods except the proposed method are similar as well as the table 3. As the larger the value of mutual information is, the more information of the fusion images obtained from source images, the better the effect of fusion there is, so doctors can see more information of both bone and tissue to apply the clinical applications, which is more useful in medicine. Moreover, compared with other nine methods, the methods NSCT and NSCT+PCNN are more time-consuming.

From the above analysis, we can draw the conclusion that the fused image of our method is superior to others in the filed of medical image fusion, in addition, the following conclusions can be drawn:

(1) Our method can manage various types of medical images from the experiments above.

(2) The fused images of the proposed method are superior to m-PCNN in extracting the main and detailed information from source images.

(3) The fused images of the proposed method can describe the information of contours and edges.

(4) The proposed method provides better performance than others in medical image processing.

(5) In practical applications, the proposed method can meet clinical demands completely.

In a word, the above four group simulation experiments show that the proposed method is more flexible than other nine methods in both subjective visual effects and objective evaluation criteria.

 Copyright ⓒ 2016 SERSC

5. Conclusion

Medical image fusion plays an important role in clinical applications. But there are many technical problems to be solved of the current medical image fusion. In this paper, a novel medical image fusion is proposed, which is based on m-PCNN and non-subsampled contourlet transform. The low- frequency and high-frequency sub-bands of the two source medical images by using the NSCT transform are obtained and two different rules are implemented to preserve more information in the fused image. The low- frequency bands are fused by using the average rules, while high-frequency coefficients are fused by inputting to the m-PCNN. The experimental results show that the proposed method outperforms the other methods by mutual information. it can not only overcome the defects which can't deal with various types of medical images, and can retain the clear region and feature information of multimodal image. In practical application, the proposed method is more useful for doctors than others mentioned above.

Acknowledgements

The work was supported by National Natural Science Foundation of China (Grant No: 61261043) and Natural Science Foundation of Ningxia (Grant No: NZ13084).

Reference

[1]Fang Yong,Liu Sheng-Peng, Infared Image Fusion Algorithm Based on Contourlet Transform and Improved Pulse Coupled Neural Networks,China Patent 1873693A,December (2006).
[2]H.li.B.Manjunach,S.Mitra, Multisensor image fusion using the wavelet transform. Graph.. Models Image Process.57,3,(1995)235-245.
[3]li M,Cai W,Tan Z, Pulse coupled neural network based image fusion. In: Prroceedings of the 2nd International Symposium on Neural Networks Springer.Chongqing,China(2005),May 30 . pp.741-746
[4]F. Nencini,A.Garzelli,S.Baronti,L.Alparone, Remote sensing image fusion using the curvelet transform. Inform Fusion 8,2(2007)143-156.
[5]Q.Zhang, B.Guo, Multifocus image fusion using the nonsubsampled contourlet transform, Signal Process.89,7(2009)1334-1346.
[6] J. Zhuqing, S. Jintao, X. Baoguo, Novel multi focus image fusion method in nonsubsampled Contourlet transform domain, Journal of Zhejiang University(Engineering Science),44,7(2010).
[7] R. Eckhorn, H.J.Reitboeck, M. Arndt, P.W. Dicke. Feature linking via synchronization among distributed assemblies: Simulation of results from cat cortex, Neural Computation,2,3 (1990): 293–307.
[8] J. L. Johnson, M. L. Padgett, PCNN models and applications. IEEE Transactions on neural networks,10, 3(1999).
[9] H. S. Ranganath, G. Kuntimad, J. L Johnson, Pulse coupled neural networks for image processing, 1995 IEEE Southeast Con, Raleigh, NC. (1995): 37-43.
[10] R. P. Broussard, S. K. Rogers, M. E. Oxley, G. L. Tarr, Physiologically motivated image fusion for object detection using a pulse coupled neural network, IEEE Transactions on Neural Networks, 10,3(1999).
[11] Wei Li, Xue-Feng Zhu, A New Image Fusion Algorithm Based on Wavelet Packet Analysis and PCNN. Proceedings of the Fourth International Conference on Machine Learning and Cybernetics, (2005); Guangzhou, China.
[12] L.Meili, L. Yanjun, W, Hongmei, Multi-focus image fusion method based on contourlet transform. Comput. Eng. Appl, 45,10(2009): 20-22.
[13] Do M N, A directional multiresolution image representation, IEEE International Conference on Image Processing, (2002) 357-360; Urbana, IL, America .
[14] Wang Z B, Ma Y D. J. Medical image fusion using m-PCNN. Information Fusion. 9,2(2008).
[15] J. L. Johnson, H. S. Ranganath, G. Kuntimad, H. J Caulfield, Pulse coupled neural networks, in:O.Omidvar, J. Dayhoff(Eds), Neural Networks and Pattern Recognition, (1998).
[16] J. L. Johnson. D. Ritter, Observation of periodic waves in a pulse coupled neural network, Optic Letters. 18,15(1993):1253-1257.
[17] Al. Da Cunha, J. Zhou, M, N. Do, The upsampled Contourlet transform: theory, design, and applications, IEEE Trans. Image Process. 15,10(2006): 3089-3101.
[18]Johnson J L,Padgett M L. PCNN models and applications. IEEE Transactions on Neural Networks,10,3(1999):480-498.
[19] Do M N, Vetterli M, An efficient directional multiresolution image representation. IEEE Transactions on Image Processing. 14,12(2005): 2091-210.

Copyright ⓒ 2016 SERSC

Copyright ⓒ 2016 SERSC